EVLA Beam Holography take 2

W. D. Cotton (NRAO) and R. Perley (NRAO) April 25, 2017

***Abstract*—This memo described the analysis of EVLA beam holography measurements at S, C and X band and an attempt to correct targeted data made in conjunction with the holography. Results are disappointing, linear polarimetry failed entirely. At C band, corrections improved the residual instrumental Stokes V due to the beam squint; Stokes I corrections made no improvement at C band and degraded the measurements in X and S band.**

***Index Terms*—Radio Beam Holography**

I. Introduction

ASYMMETRIES in gain of alt-az mounted antennas can cause artifacts in wide-field images as the beam rotates on the sky due to changing parallactic angle. Furthermore, the polarization response of the antennas vary with location in the gain pattern and these also rotate on the sky with parallactic angle. If the varying antenna response with angle ("Beam") is know it can be used to correct derived images.

The direct way to determine the antenna beam patterns is by use of holography where one antenna of a baseline is held centered on a know source of emission and the other is driven in a pattern to sample the beam. The interferometer visibility then maps the voltage beam. Wideband holography measurements have been made of the EVLA in all of its observing bands. This memo describes the derivation of frequency dependent beam images and an attempt to use them in correcting the antenna pattern. A previous set of beam measurements are reported in [1]. Examples shown here use the Obit package ([2], http://www.cv.nrao.edu/∼bcotton/Obit.html).

II. Antenna Beam Correction

Antenna beam images can be described either in terms of the Stokes parameters ("I", "Q", "U", "V") or in terms of the interferometer correlations ("RR","LL","RL","LR" for circular feeds, "XX","YY","XY","YX" for linear). In the following development the latter are used and the description is for circularly polarized feeds. The following also assume that a single, average beam image describes all antennas.

Images can be derived in a time dependent fashion correcting for the antenna pattern but this has the disadvantage that the noise in the derived image is nonstationary and increases in regions where the gain decreases. The following uses a different approach in which the dirty/residual Stokes I images are made and minor cycle cleaning are done without including the effects of the beam but the difference between the true beam and a symmetric approximation to the true beam is corrected in the calculation of the visibility sky model in each major cycle. This correction is made by modifying the Stokes I CLEAN model for the two orthogonal, parallel hand correlations (RR and LL for circular feeds) in a time and frequency dependent fashion. The EVLA offset cassigrain feeds introduce a large off–axis Stokes V instrumental term which is also corrected using separate CLEAN models for RR and LL correlations. Thus, the actual antenna beam is corrected to the symmetrized beam in the sky model subtracted from each of the parallel hand correlations each major cycle. Using multiple major cycles drives the sum of the Stokes I CLEAN components at a given pixel to the value that would have been obtained if the true antenna pattern were the symmetric version while correcting for the instrumental Stokes V from the beam squint.

Correction for the off–axis instrumental polarizations are made once the Stokes I image is made. The instrumental polarization responses are derived from the Stokes I CLEAN components and the beam images in the relevant correlations ("RR", "LL" for Stokes V and "RL","LR" for Stokes Q and U).

Imaging uses RR and LL visibilities and forms I visibilities each major cycle. CLEAN component flux density correction factors for RR ($Rgain$) and LL ($Lgain$) at a given frequency (ν) and over a limited range of parallactic angle (χ) are given by the following for each CLEAN component :

$$R = symGain(x,y,\nu)/RRBeam(x,y,\chi,\nu)$$
$$L = symGain(x,y,\nu)/LLBeam(x,y,\chi,\nu)$$
$$Igain = 1.0/(0.5*(R+L))$$
$$VGain = Igain*(0.5*((R-L))$$
$$g^{RR} = Igain + Vgain$$
$$g^{LL} = Igain - Vgain$$

where x and y are offsets in RA and Dec from the pointing center, $symGain(x,y,\nu)$ is the symmetric beam, $RRBeam(x,y,\chi,\nu)$ and $LLBeam(x,y,\chi,\nu)$ are the true RR and LL beam images.

These gains are then applied to the CLEAN sky model to derive the values to be subtracted from the visibilities.

$$V_{RR}(t,b,\nu) = \sum_{i=1}^{n} g_i^{RR}(\chi,\nu)\ amp_i(\nu)e^{-2\pi j(x_i u_\nu + y_i v_\nu)}$$

$$V_{LL}(t,b,\nu) = \sum_{i=1}^{n} g_i^{LL}(\chi,\nu)\ amp_i(\nu)e^{-2\pi j(x_i u_\nu + y_i v_\nu)}$$

where t is time, b is baseline and amp_i is the amplitude of CLEAN component i. In Obit, this is implemented in ObitSkyModelVMBeam.c routine ObitSkyModelVMBeamUpdateModel and can be applied using task MFBeam. Corrections for Stokes Q and U are not described due to lack of suitable test beam images and data, see below.

W. Cotton is with National Radio Astronomy Observatory, 520 Edgemont Rd., Charlottesville, VA, 22903 USA email: bcotton@nrao.edu

III. HOLOGRAPHY

Holography measurements have been carried out on the EVLA in all of the observing bands and are described in detail in [3]. Thesemeasurements used strong celestial sources which were weakly polarized when available. A subset of the antennas (reference antennas) were kept pointed on the holography source and the others driven to map the antenna beams In order to minimu=ize the effects of RFI, the lower frequencies ("P","L" and "S" band) were performed in an extended configuration and to minimize resolution of the holography sources, compact configurations were used for the higher frequencies ("C", "X", "Ku", "'K", "Ka", "Q" band). The measurements used the 8 bit samplers limiting a given measurement to 2 GHz band width; multiple observations were made to cover the wider bands. The square observing patterns were chosen to have adequate sampling at the highest frequency and a large enough extent at the lowest frequency to adequately sample the aperture plane. At the high frequencies this involved dual observations, "Fine" giving fine sampling of the main response of the beam and "Coarse" giving a wider sampling on the sky. Observations also included a set of pointed scans in normal interferometry mode with the holography target at various location in the antenna pattern

/* direction cosines - from R. Perley 20 Jun 2011 Note that the projection center must be the antenna beam center, not the source.

The offsets of the holography measurements from the holography source position are given by:

$$l = cos(E_s)sin(\Delta - A)$$

$$m = cos(E_a).sin(E_s) - cos(E_s).sin(E_a).cos(\Delta - A)$$

where
$\Delta - A$ = difference in azimuth between the antenna raster pointing position and the zero-offset pointing position, and is given by the offset[0] in the EVLA pointing table divided by the cosine of the elevation)
E_s = antenna elevation of the (raster) pointing direction
E_a = antenna elevation of the zero-offset (reference) pointing direction and is given by the offset[1] in the EVLA pointing table plus the source elevation.

Data were calibrated using the Obit calibration pipeline [4]. For undetermined reasons, the polarization calibration gave poor results and derived RL and LR beam images gave unusable results.

A. Beam Image formation

Pointing offsets were measured during the observations and appear not to have been applied to the holography measurements. Thus, for each moving antenna, an average beam using the data to all reference antennas was formed in the Stokes correlations RR, LL, RL and LR. Formation of the beam images from the calibrated visibilities was done using Obit task MapBeam2. Visibilities were accumulated in a grid of cells approximating the rasters used. Beam images are normalized such that the average RR and LL value at the reference pixel (pointing position) was 1.0. These images were formed for all datasets including both the Fine and Coarse sampling. Some averaging was done in frequency to improve the SNR and each Spectral Window ("IF" in AIPSish) typically has 4 channels.

Individual antenna beams were centered by fitting a circular Gaussian in each frequency plane; images were reinterpolated to position the average of the fitted centroids at the pointing position. The various antenna beams were then averaged into a combined antenna beam. At the higher frequencies for which there were fine and coarse as well as multiple 2 GHz frequency segments; all images were combined into a single cube using the spacing of the highest frequency Fine cube and covering the extent of the lowest frequency coarse image. Where fine and coarse images overlapped, the latter were given a weight of 0.1 of the former.

Beam images have been made and analyzed for S, C and X band. A symmetrized, tabulated beam was formed from the RR and LL cubes averaging over a nuber of radial cuts and over image planes assuming that the beam scaled with frequency. This latter assumption is not completely correct but close enoough for current purposes.

The inner portions of the beam images in Stokes I and V are illustrated in Figures 1 (C Band), 2 (X Band), and 3 (S Band). These are simillar to the correspnding plots in[1].

B. Symmetrized beams

Frequency scaled, interpolated versions of the symmetrized beams are available in the ObitBeamShape class. These symmetrized, 1D beams are shown in Figure 4 as voltage beams. For reference the Jinc function for a 24.5 m uniformly illuminated disk is given for the main response of the beam. For C and X band the Jinc and tabulated beams are very close, as they ought, but the tabulated S Band beam is significantly narrower. This narrower beam is suspect as it corresponds to a uniformly illuminated dish larger than the VLA antennas.

C. Pointing variations

During the correction of antenna pointing errors it was noticed that the beam centers shift somewhat with frequency. This persists with the combined beam images. Circular Gaussians were fitted in each frequency plane for the C band RR and LL cubes and the fitted values as a function of frequency are given in Figure 5. The beams are not Gaussian shaped so the peak and size will have systematic errors but the centroid should be well measured.

These pplots show systematic variation in frequency of the pointiing center; the x (az) offsets are smaller than y (el) which show opposite slopes. Ths C band feed is near azimuth 180° so the variation in elevation many be frequency dependent beam squint.

The upper and lower halves of the frequency coverage were measured on different days but the plots in Figure 5 are relatively continious. The FWHM plots show that the beam does not exactly scale with frequency

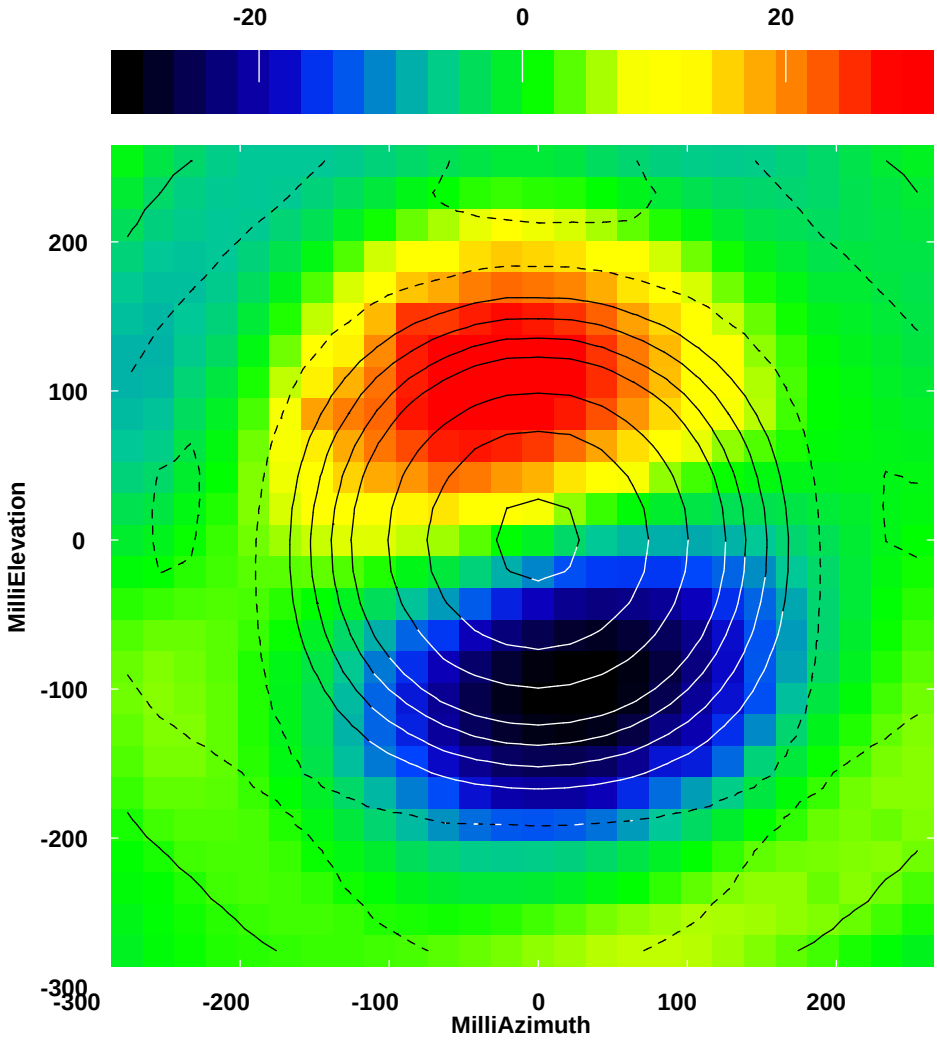

Fig. 1. Inner lobe of the C Band voltage beam at 4.9 GHz. Stokes I is given by contours at -.2,-.1,.01,.1,.2,.3,.5,.7 and 0.95. Stokes V is given in color with the scale bar at the top in units of 0.001.

IV. Pointed Observations

Having the offset pointed observations allows testing how well the derived beam shapes can be used to correct data. Since the data are snapshots, there is no significant smearing with parallactic angle and the on–axis flux density is konwn from the calibration scans. The offset observations at C band were all at the same radius and every 45° in aximuth. The offset pointings at X and S band were at a variety of offset angles. Additional pointed observations were made at X band all with the same offset radius; unfortunately, these were not fully observed and only 5 of the 8 pointings at one frequency setting were usable. Wideband images were made without and with beam corrections using Obit Wideband imaging tasks MFImage and MFBeam. Imaging produced images in each of the 16 spectral windows in the data. The results are summarized in Figures 6 - 11.

At C band (Figs.6 - 7), the measured uncorrected Stokes V agree well and the corrected images have Stokes V close to the expected vaue of 0, althoough the residuals are well above the noise. The Stokes I comparison is less good, the measured uncorrected fractional Stokes I values are only weakly correlated with the model (“Holography” line) and the agreements degraded with increasing frequency. The correction of the Stokes I value does not results in a greater agreement amoung the various samples.

At X band the offset pointings had a variable offset radius as shown in Figures 8 and 9 which makes them difficult to interpret; the model shown is for a constant radius offset. Figure 10 shows a reasonable agreement between the model and observed Stokes V but any relation for Stokes I is not apparent. At X band (Figs.8 - 10) the correlation even in Stokes V is poor and non–existant in I. The Stokes I “corrections” are rarely an improvement. The S band results (Fig.11) show the corrections to be worse than useless.

V. Beam Squint

The EVLA uses offset feeds at the casegrain focus to allow selecting the observing band by merely rotating the subreflector. This has the property of “beam squint” in which the pointing centers of the orthogonal circular beams are offset

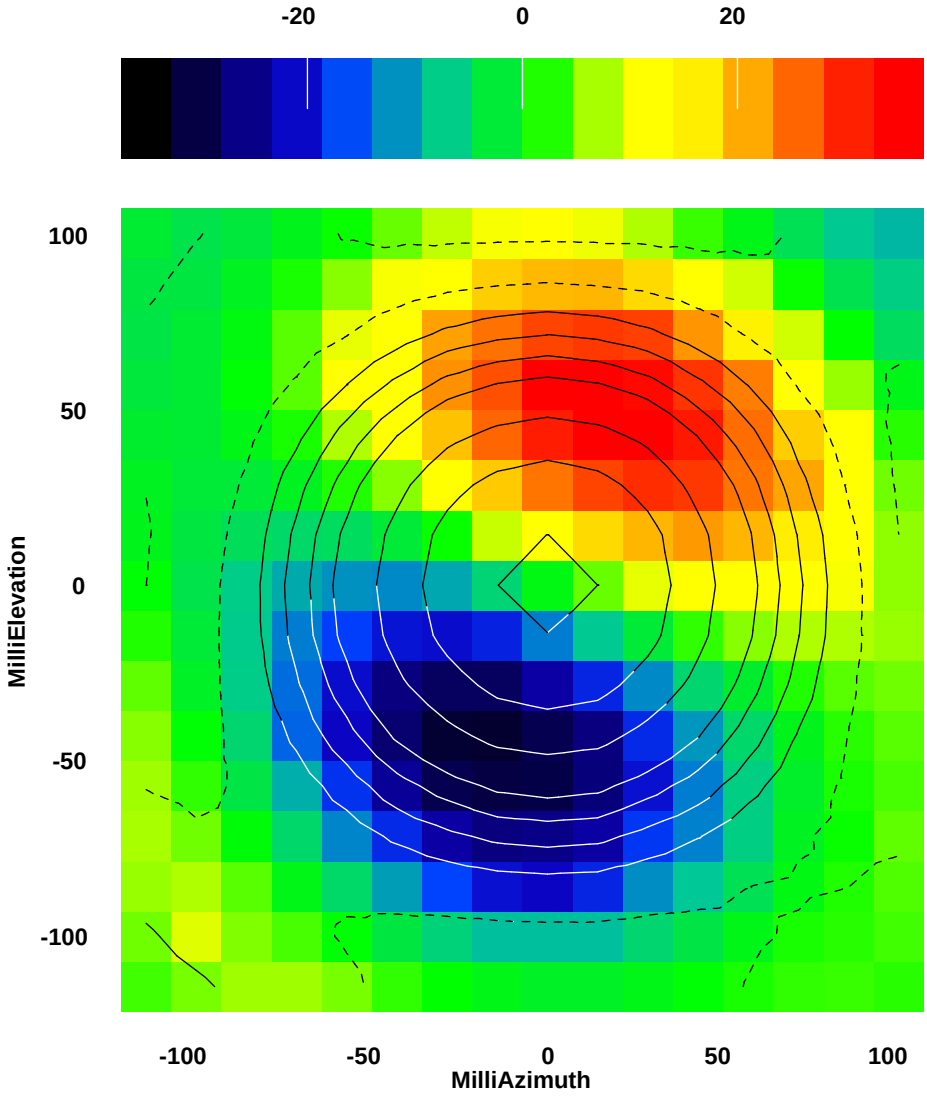

Fig. 2. Like Figure 1 but X band at 10.0 GHz.

from each other on the sky. This gives rise to the large off–axis instrumental Stokes V signal seen in Figures 6 - 11. This effect can be modeled and corrected using a parallactic angle (time) and polarization dependent pointing error [5]. The squint model and its correction applied to the same data as shown in Figure 6 spectral window 16 are shown in Figure 12. This data was imaged using Obit task Squint rather than MFBeam. Since the beam squint model assumes circularly symmetric beams in RCP and LCP, there is no correction to Stokes I. Note: Figures 6 and 12 differ in whether or not the parallactic angle is included in the “Azimuth”.

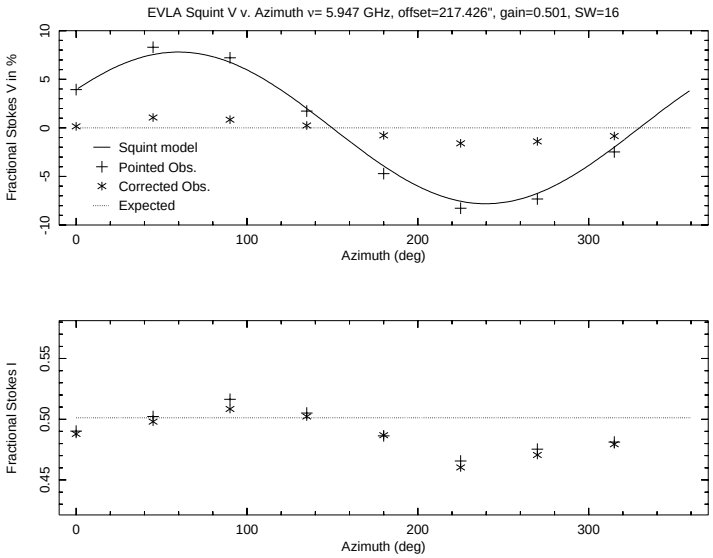

Fig. 12. Like Figure 6 but using corrections only for the beam squint.

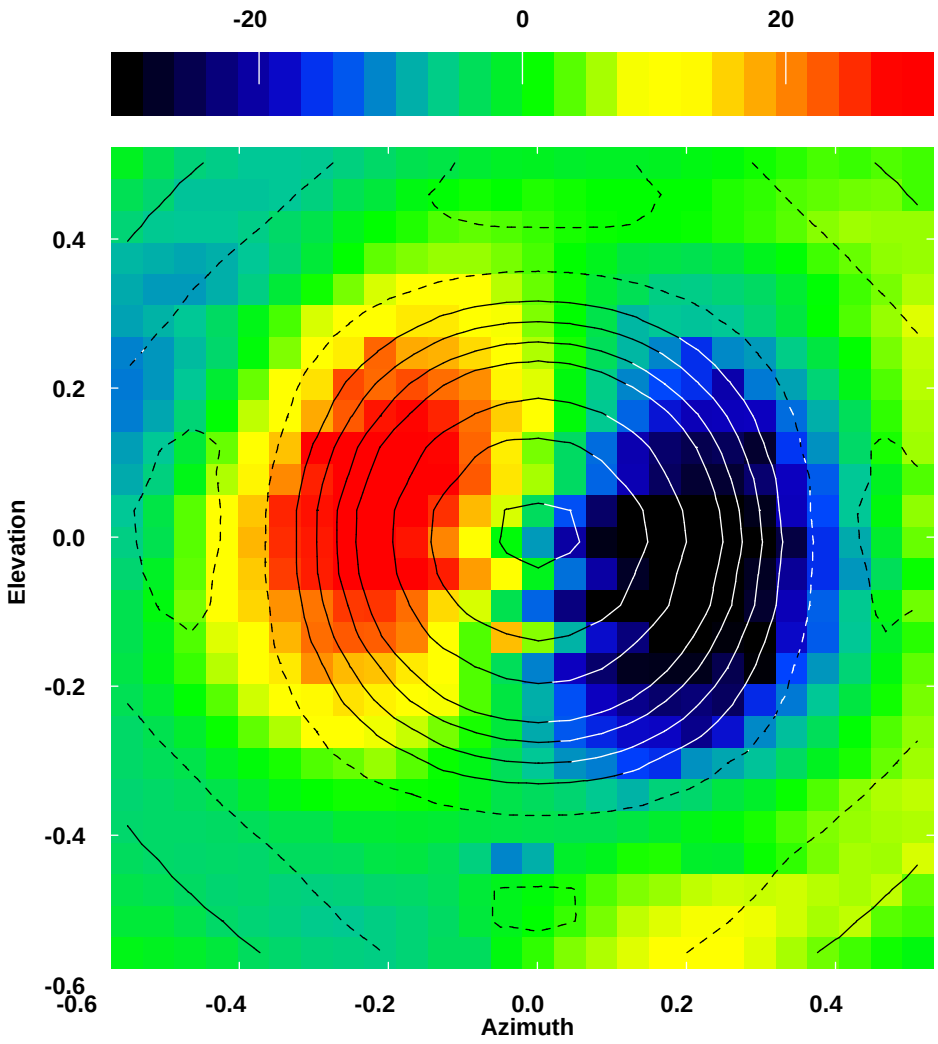

Fig. 3. Like Figure 1 but S band at 2.4 GHz.

VI. Discussion

On the whole, really disappointing. Possible the symmetrized, 1D beam shapes are useful although the S Band results brings this into question, and they do not include more than a simple scaling with frequency. Using a simple model for the beam squint resulting from the offset feeds results in a Stokes V correction which is almost as good as the holography based correction but makes no correction in Stokes I. I have no clue as to why this didn't work better, especially S band or as to why the polarimetry failed completely.

References

[1] W. D. Cotton and R. Perley, "EVLA Off-axis Beam and Instrumental Polarization," *Obit Development Memo*, no. 17, pp. 1–22, 2010. [Online]. Available: ftp://ftp.cv.nrao.edu/NRAO-staff/bcotton/Obit/EVLABeam.pdf
[2] W. D. Cotton, "Obit: A Development Environment for Astronomical Algorithms," *PASP*, vol. 120, pp. 439–448, 2008.
[3] R. Perley, "Jansky Very Large Array Primary Beam Characteristics," *EVLA Memo*, vol. 195, pp. 1–28, 2016.
[4] W. D. Cotton, "EVLA Continuum Scripts: Outline of Data Reduction and Heuristics." *Obit Development Memo*, no. 29, pp. 1–29, 2016. [Online]. Available: ftp://ftp.cv.nrao.edu/NRAO-staff/bcotton/EVLAObitScripts.pdf
[5] J. Uson and W. D. Cotton, "Beam Squint and Stokes V with Off–axis Feeds," *A&A*, vol. in press, 2008.

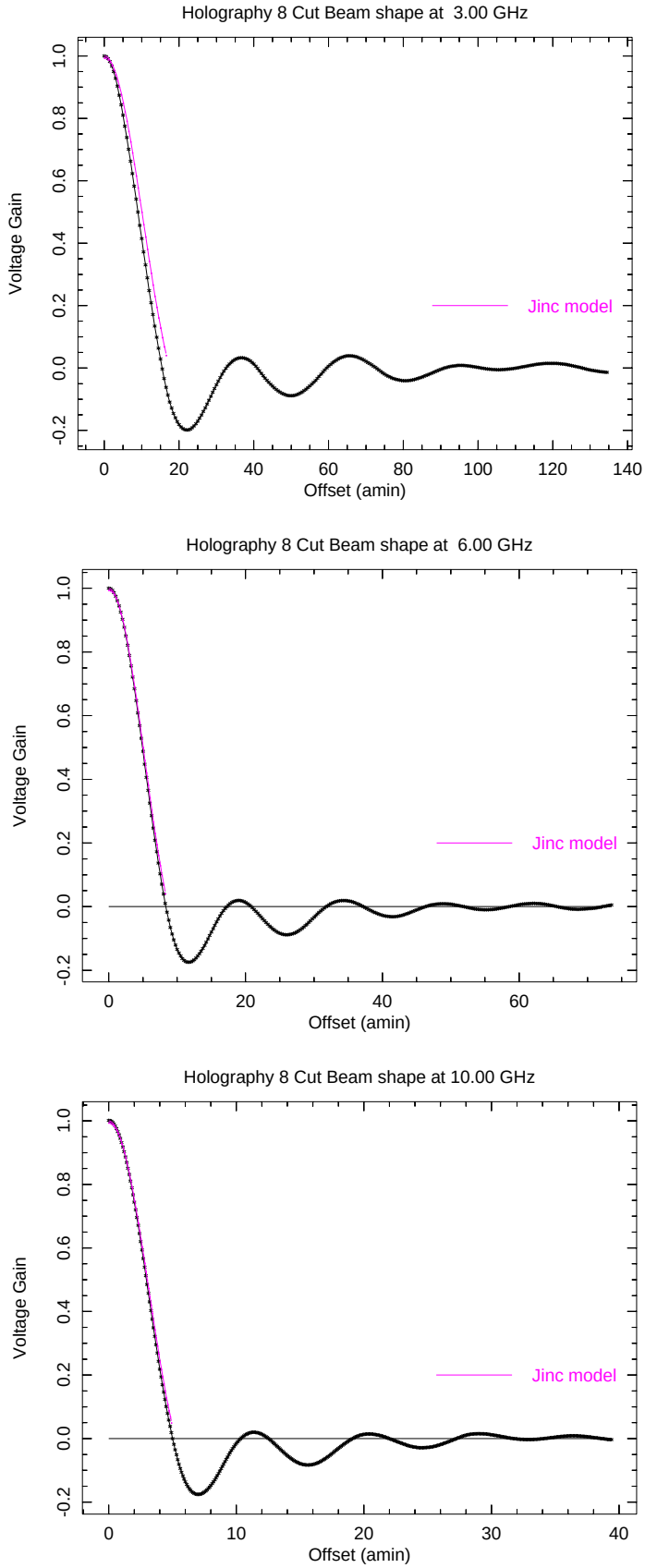

Fig. 4. Symmetrized version of the voltage beams. Top: S band, Center: C band, Bottom: X band. The approximate Jinc beam shape is given in magenta.

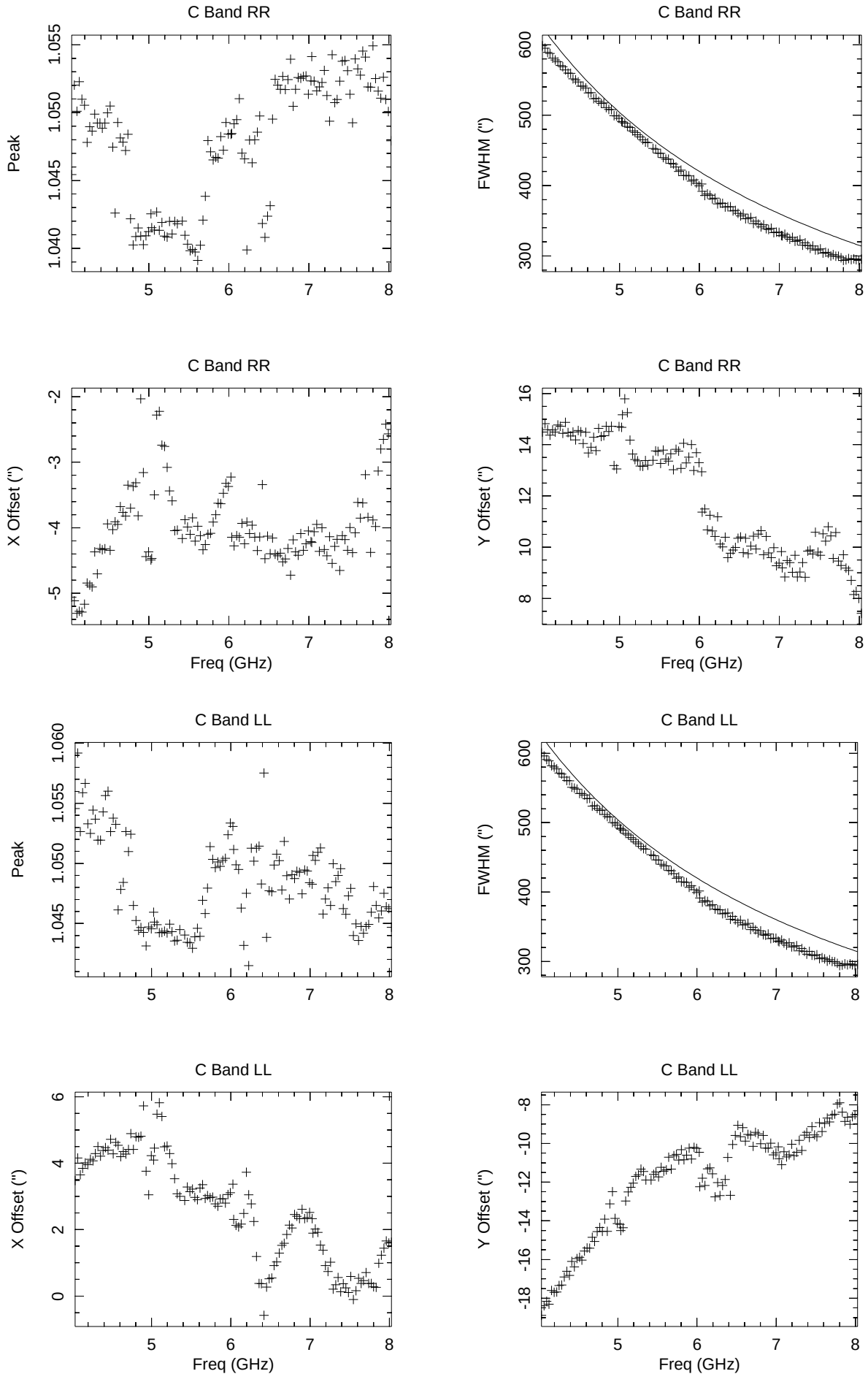

Fig. 5. Results of frequency dependent of fitting circular Gaussians to C band beam images. Upper plot is RR and lower is LL. Each panel consists of subpanels ith fitted peak, fitted FWHM, and the fitted offsets in x (Az) and y (El). The continious line on the FWHM sub panel gives the scaling in frequency

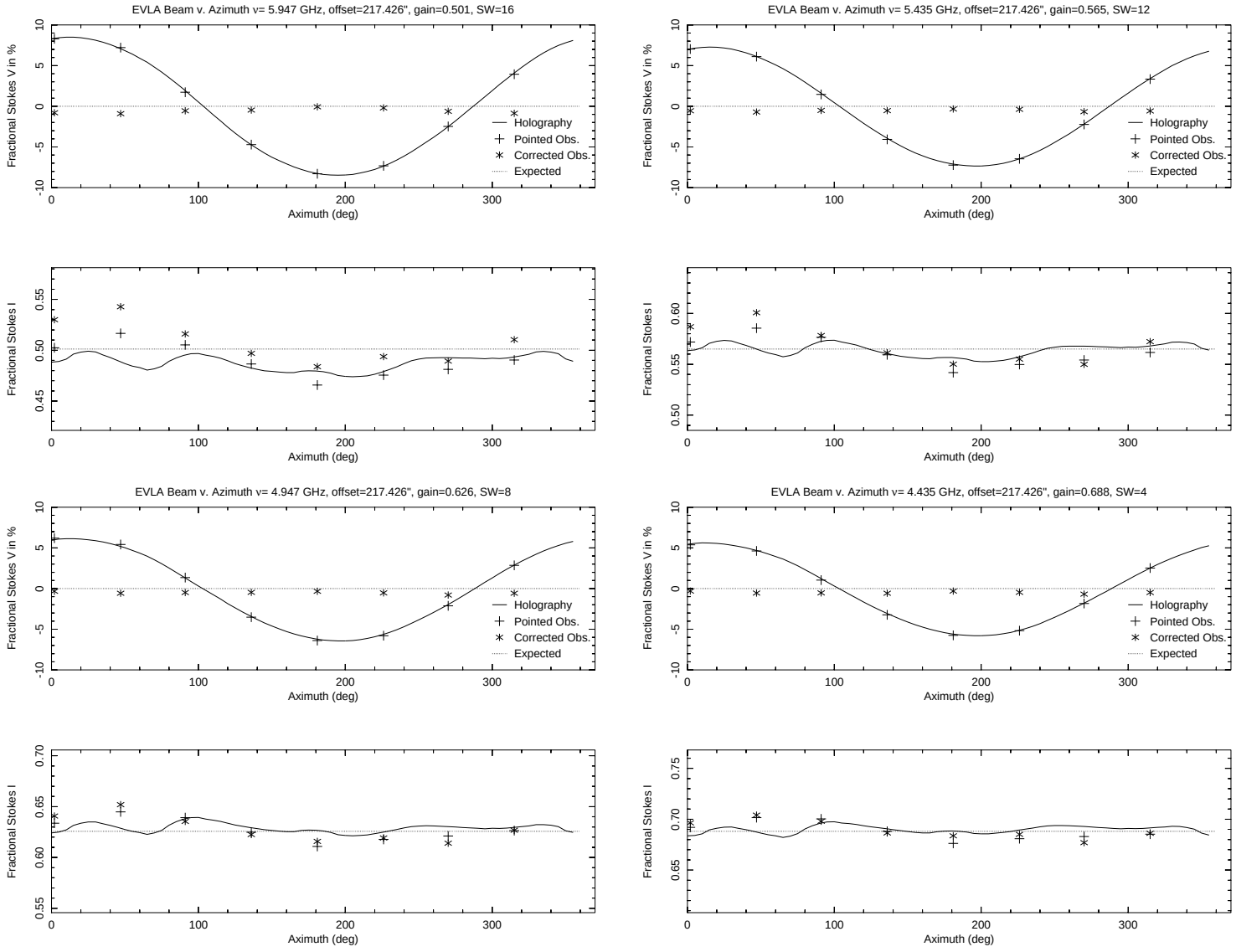

Fig. 6. Results of imaging the offset pointed observations of C band 4-6 GHz. Values of observed, corrected and model fractional Stokes V andI are given in the upper and lower panel of each plot.

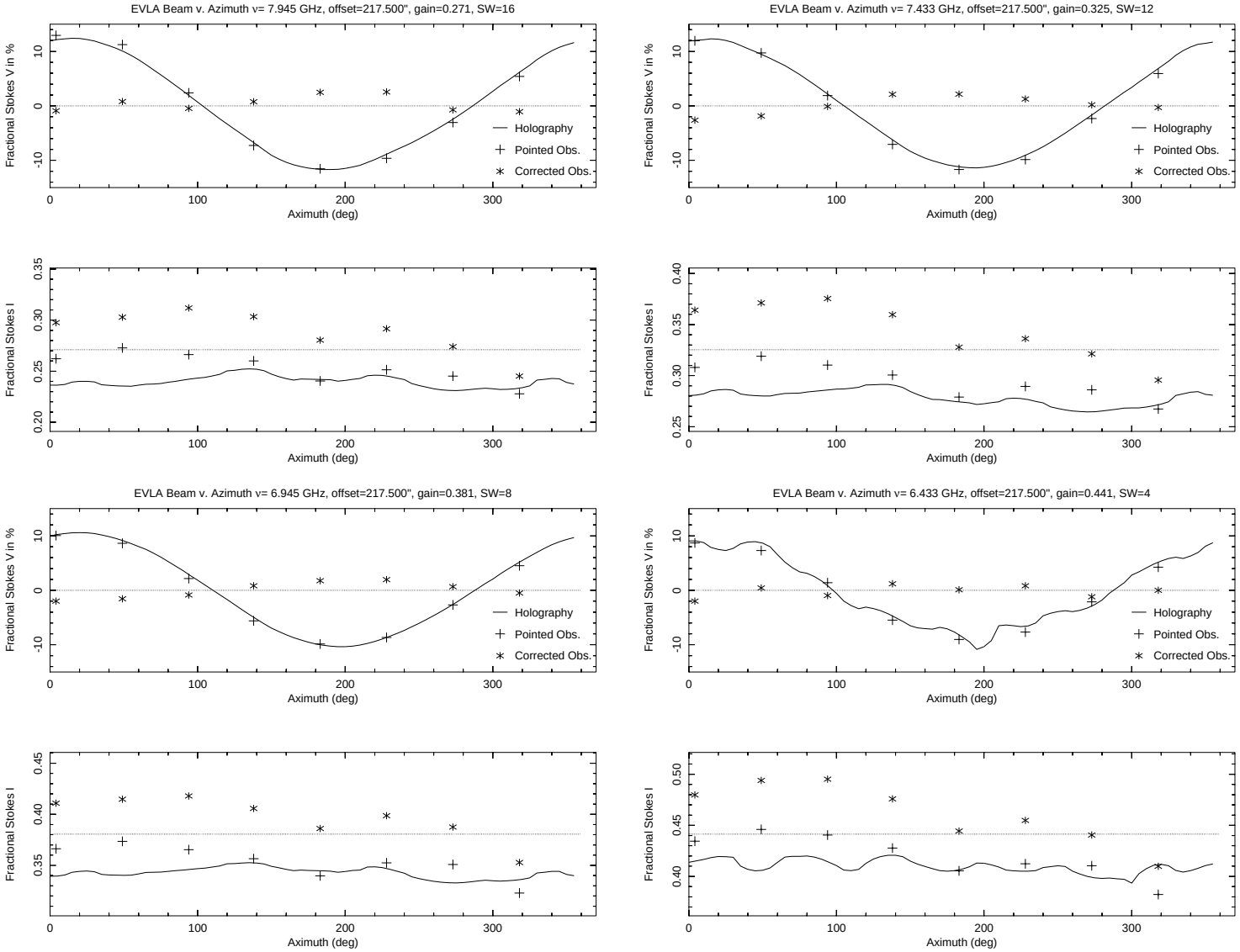

Fig. 7. Like Figure 6 but C band 6 - 8 GHz.

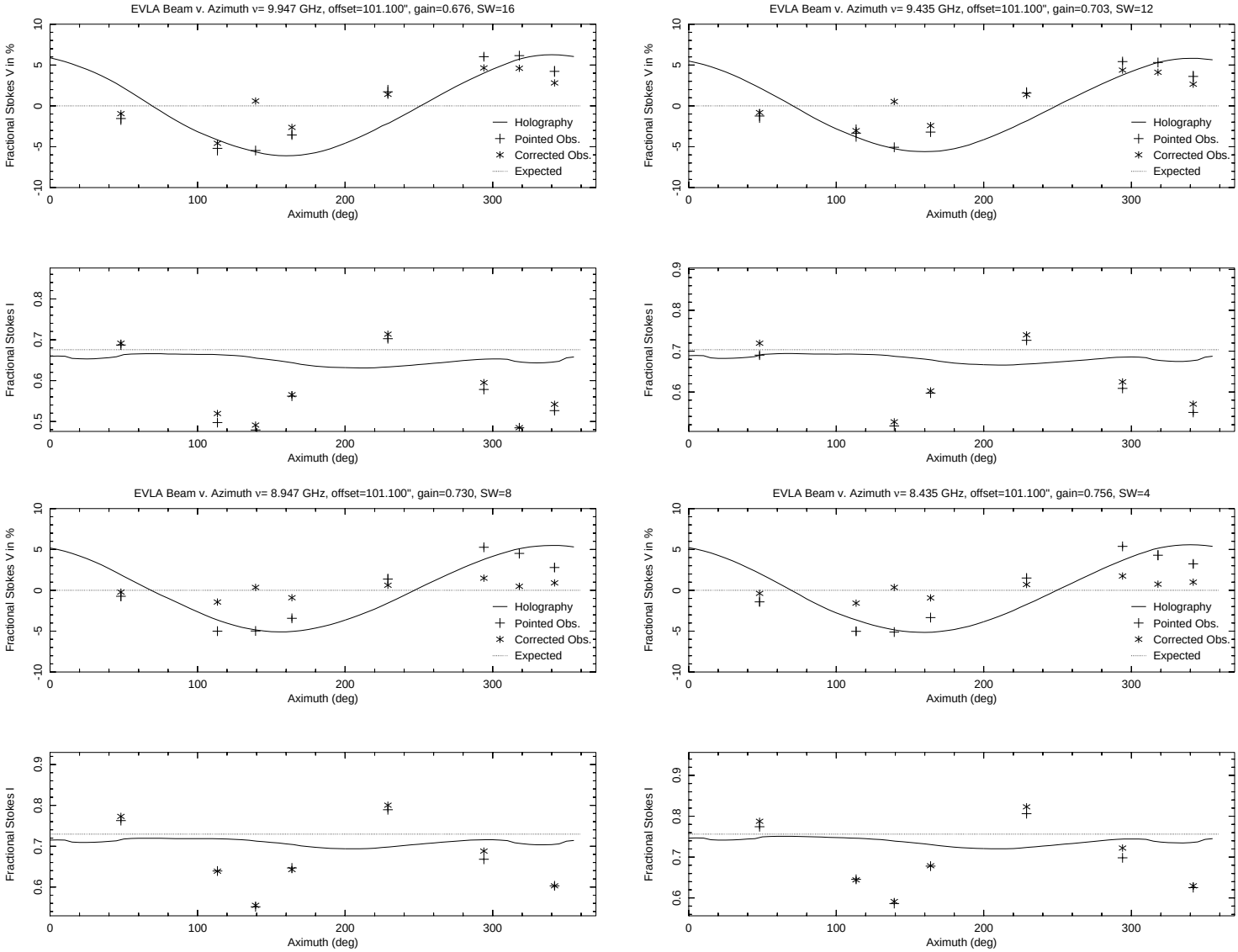

Fig. 8. Like Figure 6 but X band 8 - 10 GHz.

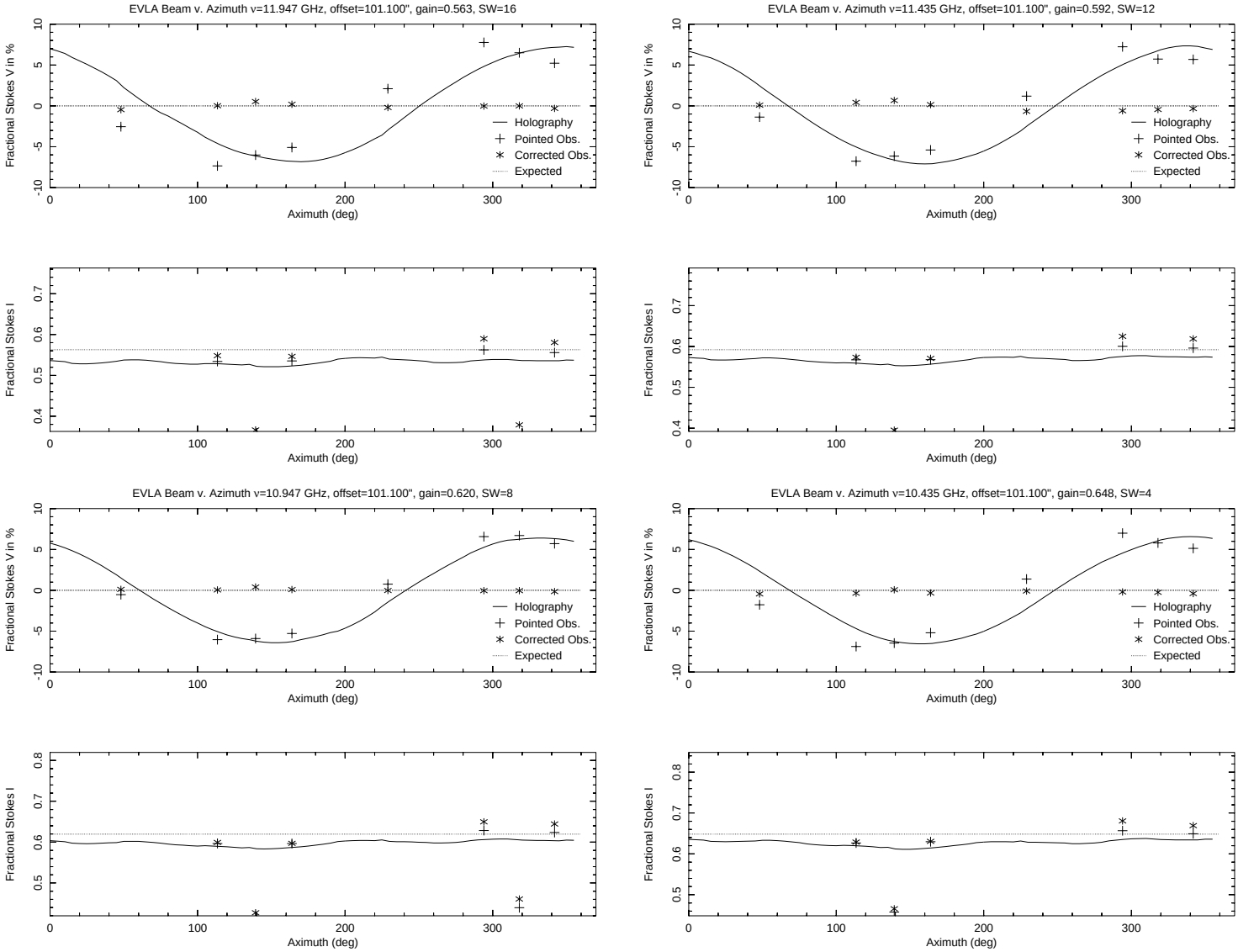

Fig. 9. Like Figure 6 but X band 10 - 12 GHz.

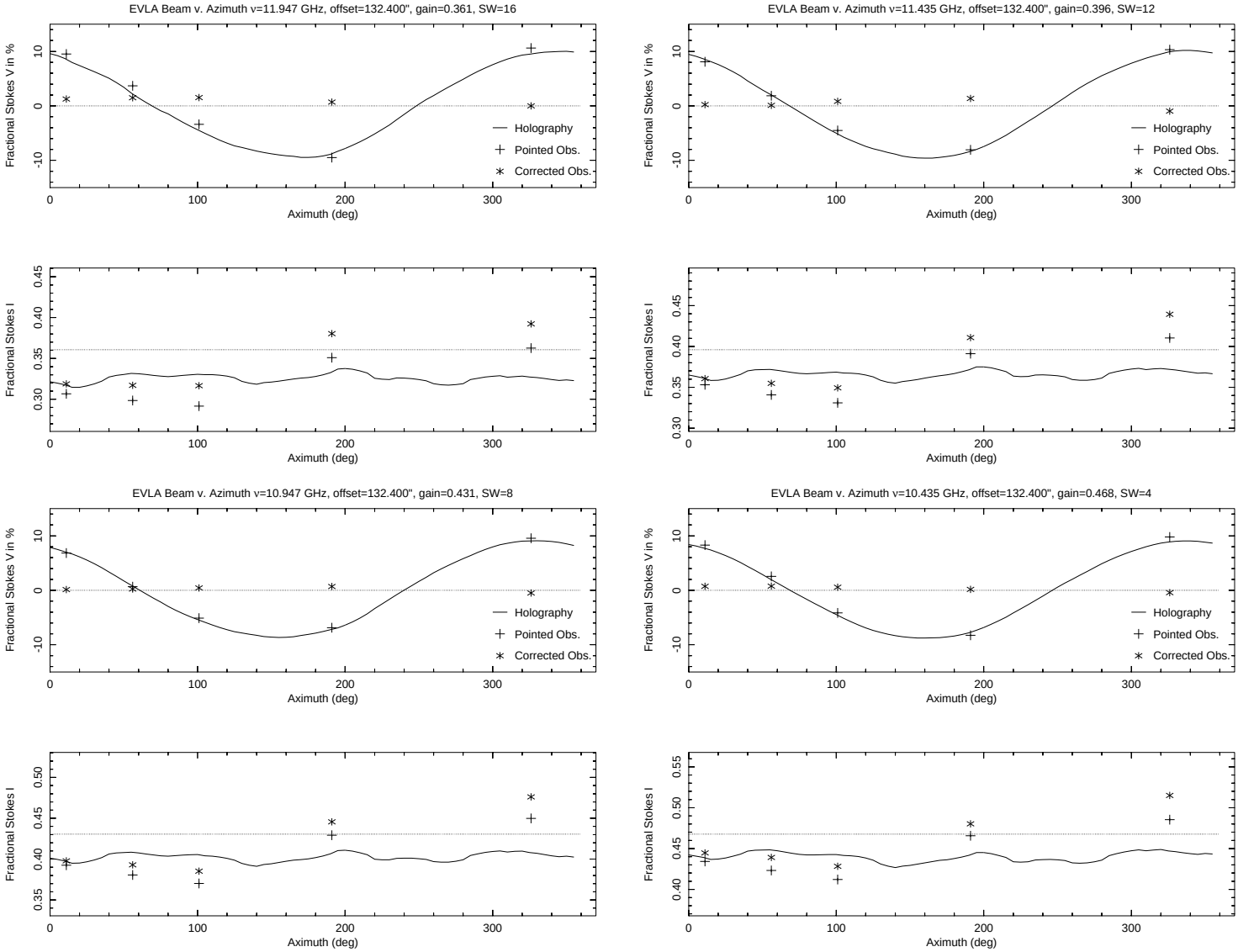

Fig. 10. Like Figure 9 but X all offsets at the same radius.

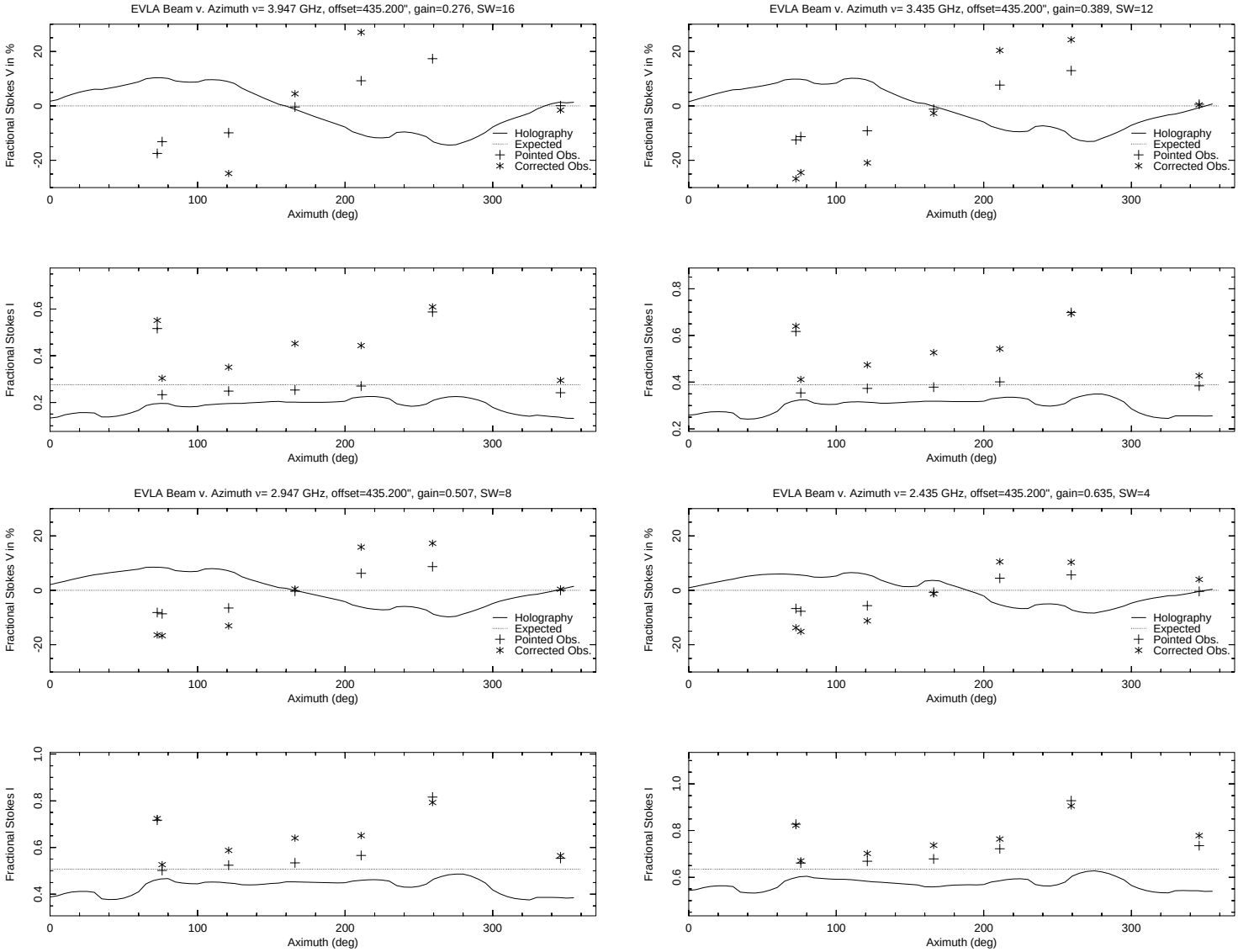

Fig. 11. Like Figure 6 but S band 2 - 4 GHz.